Rapid limb-specific modulation of vestibular contributions to ankle muscle activity during locomotion

Forbes, Patrick; Vlutters, M; Dakin, CJ; van der Kooij, Herman; Blouin, JS; Schouten, Alfred

DOI
10.1113/JP272614

Publication date
2017

Document Version
Final published version

Published in
The Journal of Physiology

The Journal of Physiology

Rapid limb-specific modulation of vestibular contributions to ankle muscle activity during locomotion

Patrick A. Forbes[1,2,6], Mark Vlutters[3], Christopher J. Dakin[4,5], Herman van der Kooij[1,3], Jean-Sébastien Blouin[6,7,8,*] and Alfred C. Schouten[1,3,*]

[1] *Department of Biomechanical Engineering, Faculty of Mechanical, Maritime and Materials Engineering, Delft University of Technology, Delft, The Netherlands*
[2] *Department of Neuroscience, Erasmus Medical Centre, Rotterdam, The Netherlands*
[3] *Laboratory of Biomechanical Engineering, Institute for Biomedical Technology and Technical Medicine (MIRA), University of Twente, Enschede, The Netherlands*
[4] *Sobell Department of Motor Neuroscience and Movement Disorders, University College London Institute of Neurology, London, UK*
[5] *Department of Kinesiology and Health Science, Utah State University, Logan, Utah, USA*
[6] *School of Kinesiology, University of British Columbia, Vancouver, British Columbia, Canada*
[7] *Djavad Mowafaghian Centre for Brain Health, University of British Columbia, Vancouver, British Columbia, Canada*
[8] *Institute for Computing, Information and Cognitive Systems, University of British Columbia, Vancouver, British Columbia, Canada*

Key points

- The vestibular influence on human walking is phase-dependent and modulated across both limbs with changes in locomotor velocity and cadence.
- Using a split-belt treadmill, we show that vestibular influence on locomotor activity is modulated independently in each limb.
- The independent vestibular modulation of muscle activity from each limb occurs rapidly at the onset of split-belt walking, over a shorter time course relative to the characteristic split-belt error-correction mechanisms (i.e. muscle activity and kinematics) associated with locomotor adaptation.
- Together, the present results indicate that the nervous system rapidly modulates the vestibular influence of each limb separately through processes involving ongoing sensory feedback loops.
- These findings help us understand how vestibular information is used to accommodate the variable and commonplace demands of locomotion, such as turning or navigating irregular terrain.

Abstract During walking, the vestibular influence on locomotor activity is phase-dependent and modulated in both limbs with changes in velocity. It is unclear, however, whether this bilateral modulation is due to a coordinated mechanism between both limbs or instead through limb-specific processes that remain masked by the symmetric nature of locomotion. Here, human subjects walked on a split-belt treadmill with one belt moving at 0.4 m s^{-1} and the other moving at 0.8 m s^{-1} while exposed to an electrical vestibular stimulus. Muscle activity was recorded bilaterally around the ankles of each limb and used to compare vestibulo-muscular coupling between velocity-matched and unmatched tied-belt walking. In general, response magnitudes decreased by ∼20–50% and occurred ∼13–20% earlier in the stride cycle at the higher belt velocity. This velocity-dependent modulation of vestibular-evoked muscle activity was retained during split-belt walking and was similar, within each limb, to velocity-matched tied-belt walking.

*These authors share senior authorship.

DOI: 10.1113/JP272614

These results demonstrate that the vestibular influence on ankle muscles during locomotion can be adapted independently to each limb. Furthermore, modulation of vestibular-evoked muscle responses occurred rapidly (∼13–34 strides) after onset of split-belt walking. This rapid adaptation contrasted with the prolonged adaptation in step length symmetry (∼128 strides) as well as EMG magnitude and timing (∼40–100 and ∼20–70 strides, respectively). These results suggest that vestibular influence on ankle muscle control is adjusted rapidly in sensorimotor control loops as opposed to longer-term error correction mechanisms commonly associated with split-belt adaptation. Rapid limb-specific sensorimotor feedback adaptation may be advantageous for asymmetric overground locomotion, such as navigating irregular terrain or turning.

(Received 15 April 2016; accepted after revision 16 December 2016; first published online 23 December 2016)
Corresponding author P. A. Forbes: Department of Neuroscience, Erasmus Medical Centre, PO Box 2040, 3000 CA, Rotterdam, The Netherlands. Email: p.forbes@erasmusmc.nl

Abbreviations CPG, central pattern generator; EVS, electrical vestibular stimulation; iEMG, integrated electromyography; mGAS, medial gastrocnemius; SOL, soleus; TA, tibialis anterior; VN, vestibular nucleus.

Introduction

Human locomotion is a complex process requiring coordination of both legs to propel the body along the desired trajectory and maintain upright balance (Misiaszek, 2006). To accommodate both tasks, sensory signals from vision, somatosensory and vestibular sources are integrated, and their contributions to locomotor muscle activity are modulated throughout the different phases of locomotion. In humans, for instance, vestibular contributions to ankle muscle activity occur primarily during the stance phase, when the foot is in contact with the floor and is most effective at contributing to balance control (Iles *et al.* 2007; Blouin *et al.* 2011; Dakin *et al.* 2013). The magnitude of this vestibulo-muscular coupling changes depending on the characteristics of the locomotor pattern, decreasing with increasing velocity and cadence (Dakin *et al.* 2013). Velocity- and cadence-dependent modulation of vestibular coupling is similar across the two limbs, which is expected given the bilateral symmetry of walking (Blouin *et al.* 2011; Dakin *et al.* 2013), and may indicate a coordinated mechanism of vestibular modulation. During everyday walking, however, we can modify the symmetry of our locomotor pattern, such as during turning or walking on uneven terrain, raising the possibility that vestibular contributions to each limb may be, at least partly, controlled independently.

Experimentally, the natural symmetry of walking can be modified to study the (in)dependence of limb locomotor control. During split-belt walking, for example, subjects walk with each foot on a separate belt which is moving at a different velocity. Humans easily adapt to split-belt walking by adjusting each limb's kinematic timing: in the fast limb stance time decreases and swing time increases, while in the slower limb stance time increases and swing time decreases (Dietz *et al.* 1994; Prokop *et al.* 1995; Reisman *et al.* 2005; Choi & Bastian, 2007). Because of these adaptations, subjects can maintain a one-to-one stepping relationship between limbs. Adaptation to split-belt walking has been proposed to involve processes targeting both limbs either independently or through coordinated bilateral actions. Adapting to one split-belt arrangement (e.g. slow–fast) does not transfer to another (opposite) arrangement, suggesting that split-belt walking is subserved by limb-specific adaptation (Prokop *et al.* 1995; Choi & Bastian, 2007). In contrast, factors common between limbs present during normal walking, such as muscle synergies (Olree & Vaughan, 1995; Ivanenko *et al.* 2006), are maintained during split-belt walking, implying that split-belt adaptation is, at least partially, bilaterally coordinated (MacLellan *et al.* 2014). Regardless of the mechanism (bilateral, unilateral or a combination of the two), sensorimotor adaptation occurs to refine limb-movement during split-belt walking (Vazquez *et al.* 2015). This adaptation presumably also involves modification of the vestibular contribution to locomotor activity. Therefore, by characterizing the adaptation of vestibulo-muscular coupling to split-belt walking we will identify how vestibular information is coordinated within each limb to suit the varying demands of walking.

The aim of the current study was to determine whether vestibular-evoked muscle responses are modulated independently within each limb or through a common influence of both limbs. We used a split-belt treadmill to control the velocity (either 0.4 or 0.8 m s^{-1}) of each limb during both tied-belt and split-belt walking tasks. Because split-belt walking typically results in limb-specific changes in cadence that differ from tied-belt conditions, subjects walked under the guidance of a metronome to control the timing of heel strike in both limbs. We quantified the vestibulo-muscular coupling in muscles acting around the

ankle using an electrically induced vestibular disturbance signal. If the vestibulo-muscular coupling in each limb is modulated independently, each limb should receive vestibular signals appropriate for that limb's kinematics. Under this assumption, we would expect to observe differences within each limb's vestibular-evoked responses only when that limb is moving at different velocities (e.g. the slower limb during split-belt *vs.* the same limb during faster velocity tied-belt conditions). Alternatively, if vestibulo-muscular coupling is modulated through bilaterally coordinated mechanisms, a bilateral response of intermediate magnitude and timing (between the fast and slow tied-belt conditions) should be expected during split-belt walking.

Methods

Ethical approval

The experimental protocol was explained prior to the experiment and all subjects gave written informed consent. The experiment conformed to the *Declaration of Helsinki* and was approved by the Delft University of Technology's Human Research Ethics Committee.

Subjects

Sixteen healthy subjects [nine men; age 27 ± 4 years, mass 74 ± 12 kg, height 179 ± 12 cm (mean ± SD)] with no self-reported history of neurological or muscular disorders participated in this study.

Stimulus

In the present study, we used a continuous electrical vestibular stimulus to deliver an isolated vestibular disturbance to subjects during all trials while they walked on a treadmill. Coupling between the vestibular stimulus and muscle activity was quantified over the walking cycle to determine the magnitude and timing of the vestibular contribution to ongoing muscle activity. Responses evoked by electrical vestibular stimulation (EVS) have been modelled (Fitzpatrick & Day, 2004) based on the anatomical distribution of afferents within the labyrinth and the assumption that both otoliths and semicircular afferents are affected by the electrical stimulus (Goldberg *et al.* 1984; Kim & Curthoys, 2004). When delivered in a binaural bipolar configuration with the head facing forward, the electrical stimulus evokes a perceived angular velocity (Peters *et al.* 2015) about an axis directed posteriorly and superiorly by 18 deg relative to the Reid's plane (Fitzpatrick & Day, 2004; Day & Fitzpatrick, 2005). During standing balance, this stimulus configuration results in a postural roll response in the frontal plane (Lund & Broberg, 1983; Britton *et al.* 1993; Mian & Day, 2014; Forbes *et al.* 2016). Although it remains unclear whether the postural responses are evoked by stimulation of both otolith and semicircular canals afferents (Mian *et al.* 2010; Cohen *et al.* 2012; Curthoys & Macdougall, 2012; Reynolds & Osler, 2012), we are only interested in the net influence of the stimulus on lower limb muscle activity and will not examine the separate contributions from the different vestibular end organs.

The electrical stimulus was provided to subjects using carbon rubber electrodes (about 9 cm^2) in a binaural bipolar arrangement. The electrodes were coated with Spectra 360 electrode gel (Parker Laboratories, Fairfield, NJ, USA) and secured over the subject's mastoid processes using an elastic headband. The electrical stimulus was delivered with an isolated constant-current stimulation unit (STMISOLA, Biopac, Goleta, CA, USA). All subjects were exposed to the same realization of the stimulus: a bandwidth-limited stochastic EVS (0–25 Hz, zero-mean low-pass filtered white noise, 25 Hz cutoff, zero lag, fourth-order Butterworth, peak amplitude of 4.5 mA, root mean square 1.1 mA) lasting either 8 or 16 min and created with Matlab software (MathWorks, Natick, MA, USA). The stimulus bandwidth (0–25 Hz) was chosen to characterize the entire frequency response of vestibular-induced modulation in lower limb muscle activity (Dakin *et al.* 2007, 2010). The stimulus amplitude was chosen to evoke a measurable muscle response while ensuring subject comfort. With the exception of three subjects, participants had never experienced EVS prior to participating in this experiment.

Protocol

Subjects walked barefoot on an instrumented split-belt treadmill with two 0.5 m wide belts (Y-Mill, Motekforce Link, Culemborg, The Netherlands) programmed to move at belt velocities of either 0.4 or 0.8 m s^{-1} (i.e. 'slow' and 'fast'). The belt velocities were chosen to replicate the conditions used by Dakin *et al.* (2013). Subjects performed baseline tied-belt conditions (both belts moving at the same velocity) first at 0.4 and then at 0.8 m s^{-1} for 8 min each (Fig. 1*A*). Following the baseline walking, subjects performed a split-belt condition for 16 min, with one belt moving at 0.4 m s^{-1} (i.e. the 'slow' limb) and the other moving at 0.8 m s^{-1} (i.e. the 'fast' limb) in order to assess the independence of vestibular coupling across limbs. The slow and fast limbs were chosen randomly across subjects. Immediately after split-belt walking, subjects performed an additional post-adaptation tied-belt condition with both belts moving at 0.4 m s^{-1} (Fig. 1*A*).

Typically, during split-belt studies walking cadence is unconstrained, and therefore subjects adopt a modified stride time (i.e. cadence) that can differ widely from

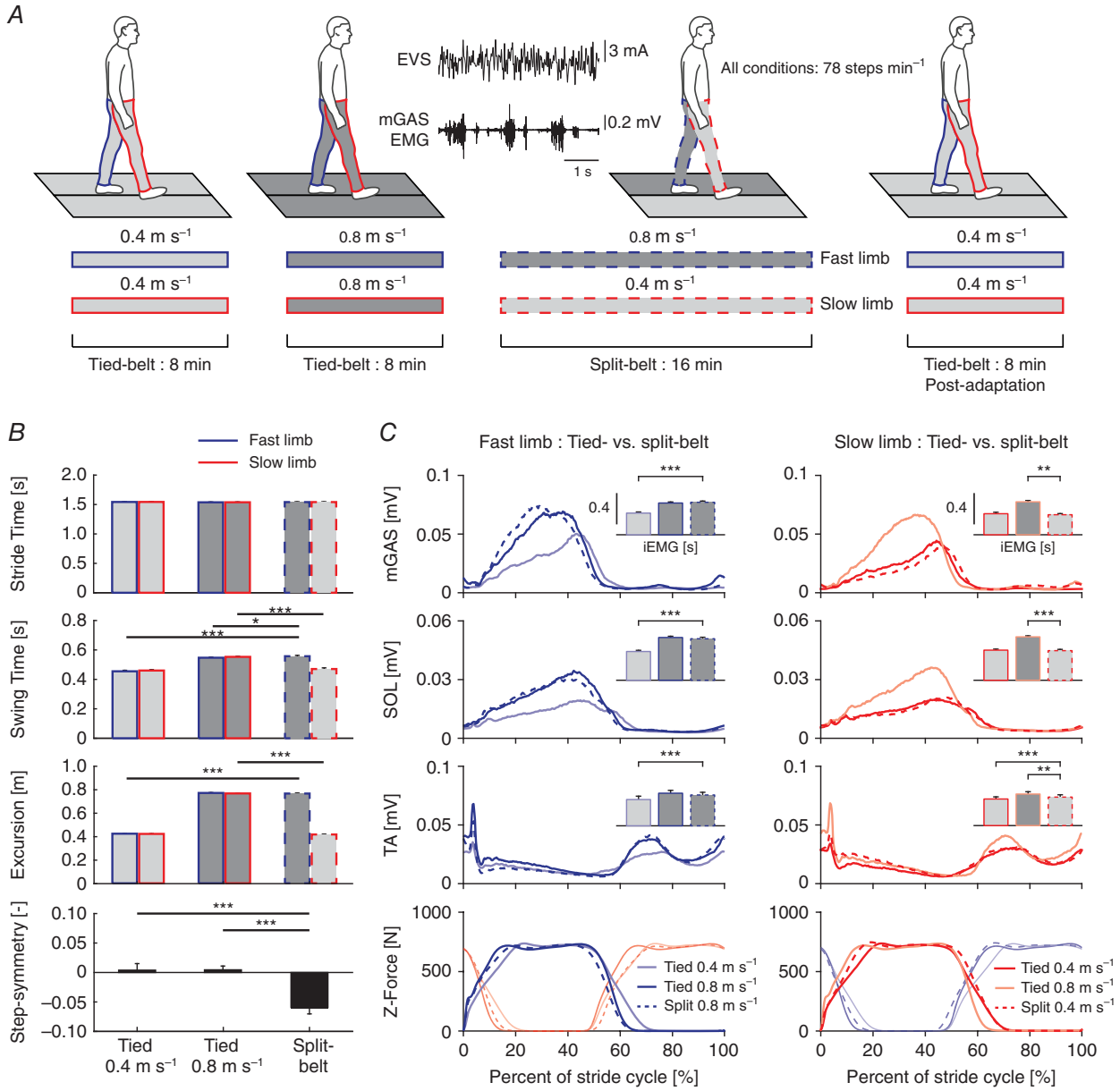

Figure 1. Experimental protocol, kinematic measures and EMG profiles
The fast and slow limb designations were defined based on the split-belt condition; during tied-belt conditions both limbs (slow and fast) moved at the same speed (i.e. 0.4 or 0.8 m s^{-1}) while their designations of 'slow' and 'fast' are maintained for comparison to split-belt responses. *A*, kinematic and EMG responses were recorded during tied-belt walking, during the adaptation (i.e. 0–8 min) and steady-state (i.e. 8–16 min) phases of split-belt walking, and during post-adaptation tied-belt walking. The horizontal grey filled bars are used to represent the different conditions and limb combinations, similar to Figs 2 and 3. *B*, group-averaged locomotion kinematic parameters (error bars represent SEM; $n = 16$) for the fast (blue) and slow (red) limbs. Significant differences (***$P < 0.001$, *$P < 0.05$) between steady-state split-belt and tied-belt conditions are shown with horizontal lines. *C*, averaged muscle activity and vertical belt force (Z-force) profiles for slow and fast limbs during the tied- (solid lines) and steady-state split-belt (dashed lines) conditions. Relative to the split-belt conditions (dashed lines), velocity-matched tied-belt responses are plotted as solid lines in the same colour and velocity-unmatched tied-belt responses are plotted as solid lines in a lighter colour (light blue and orange). Insets show the mean integrated electromyography (iEMG) and highlight significant differences (***$P < 0.001$, **$P < 0.01$) primarily between split-belt and velocity-unmatched tied-belt conditions (error bars represent SEM; $n = 16$). Phase-dependent modulation of muscle activity for each limb during the split-belt condition better matched the velocity-matched tied-belt condition. All data are aligned to the heel strike of each limb separately. For reference, shaded lines in the Z-force plot are from the contralateral limb aligned to heel strike of the respective limb. EVS, electrical vestibular stimulation; mGAS, medial gastrocnemius; SOL, soleus; TA, tibialis anterior; SEM, standard error of the mean.

both tied-belt conditions depending on the chosen belt speeds (Reisman *et al.* 2005; MacLellan *et al.* 2014). Modified cadence is known to affect the magnitude of the vestibulo-motor coupling (Dakin *et al.* 2013). Therefore, we performed a pilot study with five subjects (two were also part of the main group of 16) who were instructed to walk at a self-selected pace (unconstrained cadence) in order to estimate the variation in a participant's cadence and its influence on vestibulo-muscular coupling in the medial gastrocnemius muscle in both our tied- and split-belt conditions. Mean cadence during the unconstrained 0.4 m s^{-1} tied-belt condition was 77 $\pm$ 14 steps min^{-1} and increased to 100 $\pm$ 10 and 90 $\pm$ 16 steps min^{-1} during the unconstrained 0.8 m s^{-1} tied-belt and split-belt conditions, respectively. This range of cadence was similar to that used by Dakin *et al.* (2013). Across the split-belt and tied-belt conditions, we found modulation of vestibulo-muscular coupling (EVS–EMG coherence; see *Signal analysis*). In the slow limb, for example, the peak magnitude of vestibulo-muscular coupling during split-belt walking (0.13 $\pm$ 0.04) was lower than the 0.4 m s^{-1} tied-belt condition and higher than the 0.8 m s^{-1} tied-belt conditions (0.4 m s^{-1}, 0.20 $\pm$ 0.04; and 0.8 m s^{-1}, 0.10 $\pm$ 0.02). However, the peak timing of the split-belt condition (35 $\pm$ 2% of the stride cycle, where the stride cycle of a limb is defined between two consecutive heel strikes of that limb) more closely matched the 0.4 m s^{-1} tied-belt condition (30 $\pm$ 2%), occurring later in the stride cycle relative to the 0.8 m s^{-1} tied-belt condition (18 $\pm$ 2%). Because both velocity and cadence modulate vestibulo-motor coupling (Dakin *et al.* 2013), we were unable to interpret these changes in vestibulo-muscular coupling during split-belt walking with changes in walking velocity. Consequently, all experiments were performed with subjects ($n = 16$) guided by a metronome at 78 steps min^{-1} to control the heel strike of both limbs in all walking conditions. This cadence was chosen to replicate the conditions used by Dakin *et al.* (2013).

All trials were performed while subjects received stochastic EVS and a total of 309 and 618 strides per limb were collected during tied-belt and split-belt conditions, respectively. Subjects wore a safety harness attached to the ceiling that did not provide additional support. Instructions were given for subjects to keep their eyes open and not to touch the handrails during any of the trials. Subjects maintained a relatively constant head orientation with their Reid's plane 18 deg nose up from horizontal by keeping a headgear-mounted laser on a target located 3 m in front of them. At least two experimenters were present at all times to ensure this instruction was followed. The head position was chosen to maximize the amplitude of vestibulo-motor balance responses in the medio-lateral directions (Fitzpatrick & Day, 2004; Cathers *et al.* 2005; Fitzpatrick *et al.* 2006).

Instrumentation

Ground reaction forces were measured by force plates (Motekforce Link, Culemborg, The Netherlands) integrated in the treadmill, digitized at a frequency of 2000 Hz and low-pass filtered offline (32 Hz cutoff, zero lag, fourth-order Butterworth). Surface electromyography (EMG) (Delsys Bagnoli Systems, Delsys Boston, USA) was collected bilaterally from three muscles: medial gastrocnemius (mGAS), soleus (SOL) and tibialis anterior (TA). Although these muscles probably have a stronger contribution to anterior–posterior control during locomotion compared to the medio-lateral control required to counter the vestibular disturbance induced by stochastic EVS, they contribute to medio-lateral components of ground reaction forces and torso acceleration during undisturbed walking (Pandy *et al.* 2010). More importantly, these muscles were chosen due to the sensitivity of their vestibulo-muscular coupling responses to walking velocity (Dakin *et al.* 2013). EMG signals were pre-amplified ($\times$1000), band-pass filtered (20–450 Hz) and digitized along with force-plate data at 2000 Hz using a PCI-6229 AD card (National Instruments, Austin, TX, USA) programmed using xPC-target software (MathWorks). The same card was used to generate an analog signal at 2000 Hz for synchronization with the motion capture system. Three-dimensional kinematics were recorded using a six-camera motion capture system (PTI Visualeyez, PhoeniX Technologies Inc., Vancouver, BC, Canada) at 100 Hz. A three-LED marker cluster was placed on each foot and marker data were low-pass filtered offline (4 Hz cutoff, zero lag, fourth-order Butterworth).

Signal analysis

Signal analysis was divided into two parts: (1) a locomotion analysis, evaluating limb kinematics and muscle activity, and (2) a vestibulo-muscular analysis, evaluating the coupling between the vestibular stimulus (i.e. EVS) and muscle activity (i.e. EMG). In the locomotion analysis, we used the first 8 min (i.e. 0–8 min) of split-belt walking, which we define as the adaptation phase, to evaluate the locomotor adaptation that was expected to occur. Similarly, we used the 8 min of post-adaptation tied-belt walking to evaluate the de-adaptation that was expected to occur immediately following split-belt walking. Finally, we used the second 8 min of the split-belt condition, which we define as the steady-state phase, to establish whether the kinematics and muscle activity of each limb were similar to the velocity-matched tied-belt condition. In our vestibulo-muscular analysis, we first evaluated whether the vestibular influence on muscle activity is modulated independently within each limb. For this, we compared

vestibulo-muscular coupling responses within each limb during the steady-state phase of split-belt walking to both tied-belt conditions. We then evaluated how vestibular signals contribute to the adaptation and de-adaptation of locomotor activity evoked by split-belt walking. For this we compared a group pooled estimate of the stride-by-stride changes in vestibulo-muscular coupling (see *Vestibulo-muscular coupling*) to the group mean kinematic and muscle activity changes that occurred during the adaptation and post-adaptation phases.

Limb kinematics and EMG. Force-plate data were used to identify heel strike (when vertical force exceeded 10 N) and toe off (when vertical force decreased below 10 N) for each stride. From these estimates the mean stride and swing times for each limb were calculated during both tied-belt conditions and the steady-state phase of the split-belt condition. The stance time (i.e. stride time – swing time) was multiplied by the belt velocity to estimate the limb excursion, which is defined as the distance travelled by the foot marker from heel strike to toe off. To compare muscle activity from each limb across the tied-belt and steady-state split-belt conditions, the rectified EMG was integrated (iEMG) over the stride cycle. Prior to integration, each rectified EMG signal was normalized to the maximum amplitude across the split-belt and two tied-belt conditions. Measures of limb kinematics and muscle activity (stride time, swing time, limb excursion and iEMG) were compared across walking conditions to ensure that limb behaviour in the steady-state phase of split-belt walking was not significantly different from that of the velocity-matched tied-belt conditions.

To assess the locomotor adaptation that was expected to occur within the first half (0–8 min) of split-belt walking, we calculated stride-by-stride changes in step symmetry and muscle activity using the kinematic and EMG data, respectively. Step symmetry was defined as the difference between step lengths of the fast and slow limbs, normalized to their sum for comparison across subjects (Reisman *et al.* 2005). The step length of each limb was defined as the distance between the two foot marker clusters at heel strike of that limb. The position of each cluster was calculated as the mean of the three LEDs making up that cluster. A step symmetry of 0 indicates symmetric walking and a step symmetry less than zero indicates that the slow step is longer than the fast step. Stride-by-stride changes in muscle activity were evaluated using iEMG as well as the timing of peak muscle activity obtained from the rectified and low-pass filtered (80 Hz cutoff, zero lag, fourth-order Butterworth) EMG. At the onset of split-belt walking, the differing belt speeds evoke an initial asymmetry between left and right step lengths as well as increased muscle activity in both limbs. Over time, step lengths are gradually corrected to restore symmetric step lengths and muscle activity decreases. This adaptation of locomotion behaviour is thought to be indicative of feedforward error-correction mechanisms that occur during split-belt walking (Morton & Bastian, 2006), which, because of decreasing muscle activity, is driven in part by energy minimization (Finley *et al.* 2013). Effectively, the nervous system is hypothesized to possess an internal forward model of limb dynamics to predict the sensory consequences of movement (Kawato *et al.* 1987; Shadmehr & Mussa-Ivaldi, 1994). Deviations from this prediction are considered movement errors, which can be corrected for by modifying subsequent movements, a process that is thought to indicate the updating of the forward model to adapt the motor output to the locomotor task (i.e. walking with differing belt speeds).

To confirm that adaptation had occurred and reached a plateau during the first half (0–8 min) of split-belt walking, we examined the duration of adaptation for each subject using the methods described by Malone & Bastian (2010). Briefly, adaptation was considered complete when step symmetry in five consecutive strides fell between the range (mean $\pm$ SD) defined by the last 30 strides of the first half of split-belt walking. Because conscious correction of step asymmetries can accelerate split-belt adaptation (Malone & Bastian, 2010), we expected that by controlling cadence using a metronome the duration of adaptation would decrease compared to traditional split-belt studies. To evaluate the symmetry of walking across conditions, step symmetry was also calculated over the last 10 strides of both tied-belt conditions and the first 10 strides of the steady-state phase of split-belt walking (8–16 min). Step symmetry was also calculated over the last 10 strides of the steady-state phase of split-belt walking to determine if the asymmetry had changed throughout steady-state phase split-belt walking. We also examined the duration of adaptation from the iEMG and peak EMG timing responses with the same approach used for step symmetry. The duration of iEMG adaptation was used to confirm that muscle activity progressively decreased during adaptation (Finley *et al.* 2013; MacLellan *et al.* 2014). Both the duration of iEMG and peak EMG timing adaptation were used to examine whether changes in vestibulomotor responses were driven by general changes in muscle activity (see *Data reduction and statistical analysis*). Similarly, we estimated the duration of de-adaptation for step symmetry, iEMG and peak EMG timing during post-adaptation tied-belt walking using the same techniques used for the adaptation phase of split-belt walking.

Vestibulo-muscular coupling. To identify the expected coupling between the vestibular input stimulus (i.e. EVS) and stimulus-induced muscle activity (EMG) throughout the locomotor cycle (Blouin *et al.* 2011; Dakin *et al.* 2013), we computed the time-dependent coherence $[C(\tau,f)]$ and gain $[G(\tau,f)]$ between EVS and the rectified EMG signals

using a time-frequency approach (Zhan *et al.* 2006; Blouin *et al.* 2011) using eqns (1) and (2), respectively:

$$C(\tau, f) = \frac{\left|P_{xy}(\tau, f)\right|^2}{P_{xx}(\tau, f)\, P_{yy}(\tau, f)} \quad (1)$$

$$G(\tau, f) = \left|\frac{P_{xy}(\tau, f)}{P_{xx}(\tau, f)}\right| \quad (2)$$

where $P_{xy}(\tau,f)$ (τ and f denote the stride time and frequency, respectively) is the time-dependent cross-spectrum between the EVS and rectified EMG, and $P_{xx}(\tau,f)$ and $P_{yy}(\tau,f)$ are the time-dependent autospectra of the EVS and rectified EMG, respectively. Although coherence is more commonly used to evaluate changes in vestibulo-muscular coupling (Dakin *et al.* 2007, 2013; Reynolds, 2010, 2011; Luu *et al.* 2012; Forbes *et al.* 2014), we also evaluated gain to ensure that coherence was not modulated (i.e. decreased) simply because of the increase in non-vestibular input to the motoneuron pool (i.e. general increase in EMG magnitude) at higher limb velocities (Dakin *et al.* 2013). Gain, unlike coherence, is not normalized by the EMG power spectrum and therefore is not expected to decrease even if non-vestibular input leads to increasing EMG magnitude. Similar to previous studies (Blouin *et al.* 2011), we found that the magnitude and timing of gain and coherence were similarly modulated throughout the stride cycle and across the three walking conditions (0.4 and 0.8 m s^{-1} tied-belt and steady-state split-belt). This suggests that vestibular response amplitudes are not purely dependent on the level of excitation of the motoneuron pool. As a result, we present only the coherence data to describe changes in vestibulo-muscular coupling.

Time-dependent coherence was calculated using the continuous Morlet wavelet decomposition. Prior to estimating coherence, both EVS and EMG signals were cut into strides synchronized on the heel strike of each limb separately. Therefore, all figures depicting responses across the locomotion cycle are specific to the stride cycle of each limb (i.e. the fast and slow limb). We chose to align the data on each limb's heel strike to provide a comparable measure of coherence timing across all conditions within a limb. To avoid distortion in the coherence estimates at either end of the signals, each stride was padded with data from the previous (50%) and subsequent (50%) strides. EMG signals were full-wave rectified (Dakin *et al.* 2014) and both EVS and EMG were low-pass filtered (80 Hz cutoff, zero lag, fourth-order Butterworth) and resampled at 200 Hz. To account for stride-to-stride variability, stride duration was normalized in time by resampling the data with respect to the average stride duration across trials. This stride duration normalization was performed on the autospectra of stochastic EVS and EMG, as well as on their cross-spectrum.

From our data, it is not possible to track vestibulo-muscular coupling throughout the adaptation phase with a stride-by-stride resolution, since it has been previously shown that this would require data from approximately 225 subjects to obtain a reliable estimate of EVS–EMG coherence for each stride (Blouin *et al.* 2011). Nevertheless, by averaging data from all 16 subjects over a window of 15 strides, we were able to evaluate a single group-pooled estimate of vestibulo-muscular coupling using 240 stride cycles per window (16 subjects × 15 strides). We used an overlapping moving window to estimate the stride-by-stride changes in EVS–EMG coherence throughout walking and acknowledge that coherence from each stride window reflects an average over 15 strides that aligns with the median stride within each window. This group-pooled estimate of stride-by-stride vestibulo-muscular coupling was used to assess the vestibular contribution to muscle activity during the adaptation phase of split-belt walking and the post-adaptation phase of the subsequent tied-belt condition. The duration of adaptation of peak coherence magnitude and timing was estimated with a similar approach as used for step symmetry. To account for the increased variability associated with the pooled estimate of coherence, the number of steps used to estimate the range (mean ± SD) of adaptation completion was expanded from 30 to 50 strides.

Data reduction and statistical analysis

Limb kinematics and EMG. The limb kinematics and EMG of split-belt walking were first analysed to verify that the locomotion characteristics during the steady-state phase (8–16 min) of split-belt walking were equivalent to the velocity-matched tied-belt conditions. Comparisons were made across the steady-state split-belt and the two tied-belt conditions using a one-way repeated-measures ANOVA on all limb-specific kinematic and EMG parameters (swing time, limb excursion and iEMG) and step symmetry. When significant differences were observed, we performed pairwise comparisons (paired *t*-tests, Bonferroni corrected) to decompose the main effect between the steady-state split-belt and each tied-belt condition. Because cadence was controlled using a metronome during all conditions, we expected to observe significant limb-specific differences in locomotion behaviour between split-belt and velocity-unmatched tied-belt conditions [e.g. slow (0.4 m s^{-1}) split-belt limb *vs.* the same limb during 0.8 m s^{-1} tied-belt] but not for velocity-matched tied-belt conditions [e.g. slow (0.4 m s^{-1}) split-belt limb *vs.* the same limb during 0.4 m s^{-1} tied-belt]. A separate paired *t*-test was also used to compare step symmetry at the beginning and end of the steady-state phase of split-belt walking to confirm that subjects maintained a consistent walking pattern.

Vestibulo-muscular coupling. EVS–EMG coherence was used to identify the phase-dependent coupling between stochastic EVS and muscle activity throughout the locomotion cycle. Significant coupling was defined on a subject-by-subject basis as phases in the stride cycle when EVS–EMG coherence exceeded a confidence limit set at $P = 0.01$ using the number of strides ($n = 309$). This corresponds to a coherence of 0.015 and was chosen because it better represents an α-level of 0.05 given the bi-dimensional (time–frequency) nature of these correlations (Blouin *et al.* 2011). We extracted the magnitude and timing of the peak time-dependent coherence across all frequencies during the stance phase only. These two parameters are thought to reflect the functional contribution of a muscle's response to a vestibular disturbance over the locomotor cycle (Blouin *et al.* 2011; Dakin *et al.* 2013). We limited our analysis to the stance phase because EVS–EMG coupling in the measured ankle muscles is modulated with belt velocity primarily during this locomotion phase (Dakin *et al.* 2013).

Repeated-measures multivariate ANOVA was used to test for significant differences across the three walking conditions (0.4 and 0.8 m s^{-1} tied-belt and steady-state split-belt) using the magnitude and timing of peak coherence for all muscles within each limb. When significant differences were observed, we performed multivariate *post hoc* analyses using paired Hotelling's *t*-square tests (Bonferroni corrected) to decompose the main effect between the steady-state split-belt and each tied-belt condition. Across the two tied-belt conditions, we expected to find velocity-dependent EVS–EMG coupling similar to what has been reported previously (Dakin *et al.* 2013). For each multivariate *post hoc* that was significant, we also determined whether this difference was caused by peak coherence magnitude, timing or both using a univariate analysis (Bonferroni corrected). If, as we hypothesize, the vestibular contribution to lower limb muscle activity is modified within each limb independently, we anticipated significant differences between only velocity-unmatched split-belt and tied-belt responses [i.e. the slow (0.4 m s^{-1}) split-belt limb *vs.* the same limb in the 0.8 m s^{-1} tied-belt condition, and the fast (0.8 m s^{-1}) split-belt limb *vs.* the same limb in the 0.4 m s^{-1} tied-belt condition]. In contrast, if the vestibular contribution is modulated through bilateral action of the limbs then we anticipated significant differences between split-belt and both tied-belt responses. A significance level of 0.05 was used for all analyses and all statistical tests were performed using SPSS22 (IBM, Armonk, NY, USA).

Finally, we compared the group-pooled estimates of EVS–EMG coupling with step symmetry, iEMG and peak EMG timing responses during the adaptation and post-adaptation phases. We extracted the magnitude and timing of peak coherence from both limbs during the stance phase for each pooled stride window (15 strides) and plotted these, together with step symmetry, iEMG and peak EMG timing, with respect to the stride number from the onset of split-belt walking. Because coherence was estimated across overlapping windows of 15 strides, the stride-by-stride coherence responses were plotted relative to the median stride number within a window, such that the first window was aligned at stride 8. Our aim was to determine if the vestibular contributions to locomotor activity are adapted over a short or long time course, where the latter is observed in step symmetry and muscle activity (Reisman *et al.* 2005; Finley *et al.* 2013). If adaptation in vestibulo-muscular coupling is due to the updating of a forward model involved in adapting step symmetry (Morton & Bastian, 2006) and/or due to general changes in EMG (magnitude and timing), then we would expect to see a similar adaptation time course in both EVS–EMG coherence and step symmetry and/or EVS–EMG coherence and muscle activity (magnitude and timing), respectively. In addition, we would expect to observe lasting effects of vestibular influences on locomotor activity after adaptation. Alternatively, if vestibular contributions to locomotor activity are modulated as part of the ongoing sensorimotor control loop to the limbs, then velocity-dependent changes in EVS–EMG coherence should occur rapidly during split-belt walking, with minimal aftereffects following adaptation.

Results

Limb kinematics and EMG during split-belt walking are gradually adapted to mimic velocity-equivalent tied-belt walking

Subjects maintained a consistent locomotor pattern in time with the metronome and did not lose balance during all trials, despite the presence of stochastic EVS or the locomotor adaptation required for split-belt walking. For all subjects, step symmetry plateaued within the first 8 min of split-belt walking (mean 128 strides $\approx$ 3 min, range 22–262 strides $\approx$ 0.5–6.7 min). Similarly, muscle activity (iEMG) progressively decreased during split-belt walking adaptation; the mean duration of adaptation varied across muscles and limb velocities, but ranged between $\sim$40 and 100 strides (Table 1). In addition, the mean duration of adaptation for the peak EMG timing ranged on average between $\sim$20 and 70 strides, also depending on muscle and limb velocity (Table 1). After the adaptation phase (0–8 min) of split-belt walking, subjects exhibited slightly asymmetric step lengths (negative mean step symmetry), unlike the near zero step symmetry observed during both tied-belt walking conditions (Fig. 1; Table 2). This asymmetry was maintained throughout the split-belt paradigm: step symmetry was not significantly different between the beginning and end of the steady-state

Table 1. Summary of the duration (number of strides) of adaptation and de-adaptation during the first 8 min (0–8 min) of split-belt walking and post-adaptation tied-belt walking, respectively

Variable			Adaptation duration (strides)	De-adaptation duration (strides)
Step-symmetry			128 ± 22	82 ± 19
Fast limb	iEMG	mGAS	86 ± 16	34 ± 4
		SOL	94 ± 18	21 ± 4
		TA	41 ± 10	54 ± 10
	Peak EMG timing	mGAS	71 ± 10	32 ± 4
		SOL	53 ± 9	37 ± 8
		TA	19 ± 4	22 ± 3
	Peak coherence magnitude	mGAS	34	13
		SOL	28	13
		TA	18	33
	Peak coherence timing	mGAS	13	22
		SOL	13	18
		TA	31	13
Slow limb	iEMG	mGAS	77 ± 18	67 ± 14
		SOL	41 ± 7	78 ± 9
		TA	54 ± 9	32 ± 8
	Peak EMG timing	mGAS	47 ± 7	28 ± 4
		SOL	33 ± 5	28 ± 4
		TA	22 ± 6	22 ± 5
	Peak coherence magnitude	mGAS	13	17
		SOL	13	19
		TA	22	19
	Peak coherence timing	mGAS	15	14
		SOL	13	13
		TA	16	13

These duration estimates were derived from step symmetry, iEMG magnitude, peak EMG timing, peak coherence magnitude and peak coherence timing. The fast and slow limb designations were defined based on the split-belt condition; during the post-adaptation tied-belt condition both limbs (slow and fast) moved at the same speed (i.e. 0.4 m s^{-1}) while their designations of 'slow' and 'fast' are maintained for comparison with split-belt responses. Values are means ± SEM ($n = 16$) for step-symmetry, iEMG and peak EMG timing. Duration values for peak coherence magnitude and timing were extracted from the group-pooled time–frequency coherence estimates and therefore $n = 1$. mGAS, medial gastrocnemius; SOL, soleus; TA, tibialis anterior; SEM, standard error of the mean.

phase (8–16 min) of split-belt walking (beginning, −0.06 ± 0.04; and end, −0.06 ± 0.03; $t_{15} = 0.09$, $P = 0.926$). During the post-adaptation phase, asymmetry in step length washed out quickly and step symmetry plateaued after an average of 82 strides (range 10–250 strides ≈ 0.25–6.5 min). Similarly, both iEMG and peak EMG timing returned to normal levels within ∼20–80 and ∼20–40 strides, respectively, depending on muscle and limb velocity (Table 1). These kinematic and EMG responses demonstrate the typical adaptation (and de-adaptation) that is expected to occur due to split-belt walking.

Steady-state split-belt walking, and both tied-belt walking conditions, produced robust and significant changes in limb excursion and swing time across walking conditions in the fast limb and slow limb (Fig. 1; Table 2). Overall, when a limb was moving at 0.8 m s^{-1}, limb excursion was ∼82% larger and swing time was ∼20% longer relative to the 0.4 m s^{-1} velocity. *Post hoc* analyses of the fast limb responses revealed that limb excursion during split-belt walking was larger (81 ± 5%) relative to the velocity-unmatched 0.4 m s^{-1} tied-belt condition, but not significantly different from the velocity-matched 0.8 m s^{-1} tied-belt condition (Table 2). However, swing time in the fast limb during the split-belt condition was longer than both 0.4 m s^{-1} velocity-unmatched (23 ± 8%) and velocity-matched 0.8 m s^{-1} tied-belt conditions (2 ± 3%), but the difference compared to the latter was small. *Post hoc* analyses of the slow limb responses revealed that both limb excursion and swing time during split-belt walking decreased (45 ± 4 and 15 ± 4%, respectively) relative to the velocity-unmatched 0.8 m s^{-1} tied-belt condition, but were not different from the velocity-matched 0.4 m s^{-1} tied-belt condition.

Phase-dependent modulation of EMG was observed across all recorded muscles, and muscle activity generally increased at higher belt velocities (Fig. 1*C*). We found a significant effect of walking condition on the iEMG of all muscles in both the fast limb and the slow limb (Fig. 1; Table 2). *Post hoc* analyses of fast limb mGAS,

Table 2. Summary of limb kinematic and EMG values as well as their statistical tests

Variable		Tied-belt 0.4 m s^{-1}	Tied-belt 0.8 m s^{-1}	Split-belt	ANOVA and *post hoc* results				
					Walking condition		0.4 *vs.* 0.8 m s^{-1} tied-belt	Split- *vs.* tied-belt: unmatched	Split- *vs.* tied-belt: matched
					$F_{2,30}$	P			
Step-symmetry (–)		0.006 ± 0.01	0.002 ± 0.01	−0.06 ± 0.01	20.24	<0.001	*1.000*	0.001	<0.001
Fast limb	Limb excursion (m)	0.42 ± 0.003	0.77 ± 0.004	0.77 ± 0.01	5153.18	<0.001	<0.001	<0.001	*0.402*
	Swing time (s)	0.45 ± 0.01	0.55 ± 0.005	0.56 ± 0.01	167.65	<0.001	<0.001	<0.001	0.045
	mGAS iEMG (s)	0.29 ± 0.02	0.43 ± 0.01	0.44 ± 0.02	66.22	<0.001	<0.001	<0.001	*1.000*
	SOL iEMG (s)	0.39 ± 0.02	0.57 ± 0.01	0.56 ± 0.02	105.85	<0.001	<0.001	<0.001	*0.733*
	TA iEMG (s)	0.35 ± 0.04	0.44 ± 0.04	0.42 ± 0.04	17.29	<0.001	<0.001	0.015	*0.067*
Slow limb	Limb excursion (m)	0.42 ± 0.003	0.77 ± 0.004	0.42 ± 0.003	6486.74	<0.001	<0.001	<0.001	*0.404*
	Swing time (s)	0.46 ± 0.01	0.55 ± 0.01	0.47 ± 0.01	108.5	<0.001	<0.001	<0.001	*0.600*
	mGAS iEMG (s)	0.28 ± 0.02	0.44 ± 0.01	0.27 ± 0.02	64.58	<0.001	<0.001	<0.001	*0.900*
	SOL iEMG (s)	0.40 ± 0.01	0.58 ± 0.01	0.40 ± 0.02	133.14	<0.001	<0.001	<0.001	*1.000*
	TA iEMG (s)	0.32 ± 0.03	0.42 ± 0.03	0.36 ± 0.03	32.47	<0.001	<0.001	0.002	0.001

The fast and slow limb designations were defined based on the split-belt condition; during tied-belt conditions both limbs (slow and fast) moved at the same speed (i.e. 0.4 or 0.8 m s^{-1}) while their designations of 'slow' and 'fast' are maintained for comparison with split-belt responses. Values are means ± SEM (n = 16). The italicized values represent effects that were not significant.

SOL and TA muscles revealed that iEMG during split-belt walking was larger (53 ± 20, 45 ± 20 and 20 ± 20%, respectively) relative to the velocity-unmatched 0.4 m s^{-1} tied-belt condition, but not significantly different from the velocity-matched 0.8 m s^{-1} tied-belt condition (Table 2). Similarly, *post hoc* analyses of slow limb mGAS and SOL muscles revealed that iEMG during split-belt walking was smaller (39 ± 16 and 31 ± 12%, respectively) relative to the velocity-unmatched 0.8 m s^{-1} tied-belt condition, but not significantly different from the velocity-matched 0.4 m s^{-1} tied-belt condition. In contrast, the slow limb TA muscle was significantly different from both tied-belt responses, being larger (19 ± 14%) than the velocity-matched 0.4 m s^{-1} tied-belt condition and smaller (10 ± 10%) than the velocity-unmatched 0.8 m s^{-1} tied-belt condition. Overall, these kinematic and EMG responses suggest that the movement and muscle activity of the slow and fast limbs during steady-state metronome-controlled split-belt walking closely mimicked their velocity-matched tied-belt conditions.

Vestibulo-muscular coupling during steady-state split-belt walking mimics velocity-matched tied-belt walking

Consistent with previous results (Dakin *et al.* 2013), phase-dependent EVS–EMG coupling was present in all recorded muscles for all subjects (see Fig. 2 for a single subject's mGAS and Fig. 3 for the group average of all muscles). EVS–EMG coupling was prominent throughout the stance phase in all three muscles but muscle-specific variations in the timing of peak coherence were observed: peak coherence occurred early–mid stance in mGAS, mid–late stance in SOL and late stance in TA (Fig. 3).

During both tied- and split-belt walking, increasing belt velocity produced robust changes in the coupling between the EVS and muscle activity. EVS–EMG coherence from a single subject's mGAS muscles illustrates this modulation (Fig. 2). Across tied-belt conditions, walking at 0.8 m s^{-1} decreased peak coherence by 34% and advanced the timing of the peak 13% (i.e. 200 ms) earlier in the stride cycle relative to walking at 0.4 m s^{-1}. Similar velocity-dependent modulation of EVS–EMG coherence was observed during the steady-state phase of split-belt walking (i.e. 8–16 min). In the fast limb, peak coherence decreased by 52% and occurred 15% (225 ms) earlier in the stride cycle relative to the same limb during the 0.4 m s^{-1} velocity-unmatched tied-belt condition. In the slow limb, the opposite response [i.e. peak coherence increased by 50% and occurred 18% (270 ms) later in the stride cycle] was observed relative to the 0.8 m s^{-1} velocity-unmatched tied-belt condition. Coherence magnitude and timing in both the fast and the slow limbs were similar to their velocity-matched tied-belt conditions, differing by less than 18% in magnitude and 2% (35 ms) in timing.

The changes in vestibulo-muscular coupling associated with limb velocity were confirmed in the group data (Figs 3 and 4; Table 3). We found a significant effect of walking condition (0.4 and 0.8 m s^{-1} tied-belt and steady-state split-belt) for all muscles in both limbs (Table 4). When comparing between the two tied-belt velocities, *post hoc* multivariate analyses revealed that EVS–EMG coherence during 0.8 m s^{-1} tied-belt walking was significantly different from 0.4 m s^{-1} tied-belt walking.

Univariate analyses indicated that for the higher belt velocity, vestibular contributions to locomotor activity in ankle muscles (with the exception of the slow limb's SOL) decreased by ∼20–50% and occurred ∼13–20% (200–310 ms) earlier in the stride cycle (Tables 3 and 4). In the slow limb's SOL muscle, coherence magnitude did not differ across belt speeds; however, similar to all other muscles (including the same muscle in the fast limb), peak timing occurred 16 ± 11% (256 ± 181 ms) earlier in the stride cycle when walking at 0.8 m s^{-1}. These results indicate that at higher belt velocities, vestibular contributions to locomotor activity in ankle muscles decrease and occur earlier in the stride cycle.

Split-belt walking was also associated with changes in vestibulo-muscular coupling specific to the velocity of each limb. Our *post hoc* multivariate analyses revealed that EVS–EMG coherence during split-belt walking was significantly different from velocity-unmatched tied-belt conditions for all muscles in both limbs. Univariate analyses indicated that peak coherence decreased by ∼15–45% and occurred ∼13–28% (200–429 ms) earlier in the stride cycle when the limb was moving at a higher belt speed (Tables 3 and 4). As with our tied-belt comparisons, the slow limb SOL muscle was again the one exception: while coherence magnitude did not differ relative to the 0.8 m s^{-1} velocity-unmatched tied-belt condition, timing did differ and occurred 13 ± 10% (203 ± 153 ms) earlier in the stride cycle. In contrast, *post hoc* multivariate analyses revealed that EVS–EMG coupling during split-belt walking was not significantly different from velocity-matched tied-belt conditions for almost all muscles in both limbs. The slow limb mGAS muscle was the one exception and differed from both velocity-unmatched and velocity-matched tied-belt responses. Univariate analyses comparing slow limb mGAS split-belt responses to the 0.4 m s^{-1} velocity-matched responses indicated that while peak coherence during split-belt walking was 17 ± 12% lower, peak timing did not differ (Tables 3 and 4).

Vestibulo-muscular coupling is rapidly modulated during split-belt adaptation (and de-adaptation)

The onset of asymmetric belt speeds during split-belt walking produced rapid changes in vestibulo-muscular coupling during the adaptation phase (0–8 min), and when the belts were tied (0.4 m s^{-1}) in the post-adaptation phase (see Figs 5 and 6 for mGAS responses). Peak

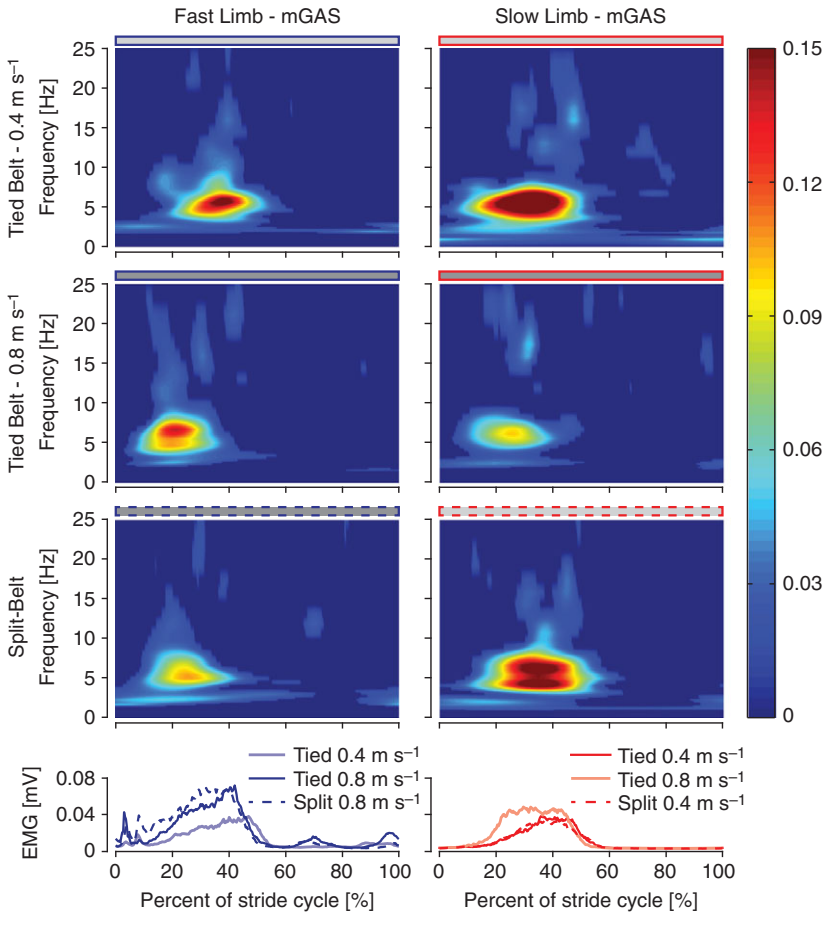

Figure 2. Coherence and EMG plots of the fast and slow limbs from an example subject's mGAS muscle during tied-belt and split-belt walking conditions
Coherence magnitude is indicated by the colour bars and for illustrative purposes data below the $P = 0.01$ confidence limit have been set to zero. Horizontal grey bars above each coherence plot are used to represent the different condition and limb combinations, similar to Figs 1 and 3. Data are aligned to the heel strike of each limb separately.

coherence magnitude demonstrated a high level of variability in both phases of walking that was probably due to the limitation that only a single estimate of stride-by-stride coherence could be obtained from our data. Nevertheless, from the onset of split-belt walking, coherence magnitude was higher in the slow limb compared to the fast limb for all muscles and remained so throughout the majority of the adaptation phase. For the mGAS muscle, peak coherence was initially low and increased to a plateau similar to peak coherence magnitude during steady-state split-belt walking within each limb (Fig. 6*C*), possibly indicating a progressive adaptation of vestibulo-muscular coupling. Changes in iEMG across the two limbs occurred rapidly at the onset of split-belt walking, and similar to coherence, plateaued to levels matching steady-state split-belt walking wherein muscle activity was always higher in the slow limb (Fig. 6*B*). Despite these similarities, however, the time course of changes in peak coherence was more rapid (~10–26 stride windows, i.e. 18–34 strides) than the duration of adaptation required for iEMG (~40–100 strides) or step symmetry (128 strides) to plateau (see Table 1 for all

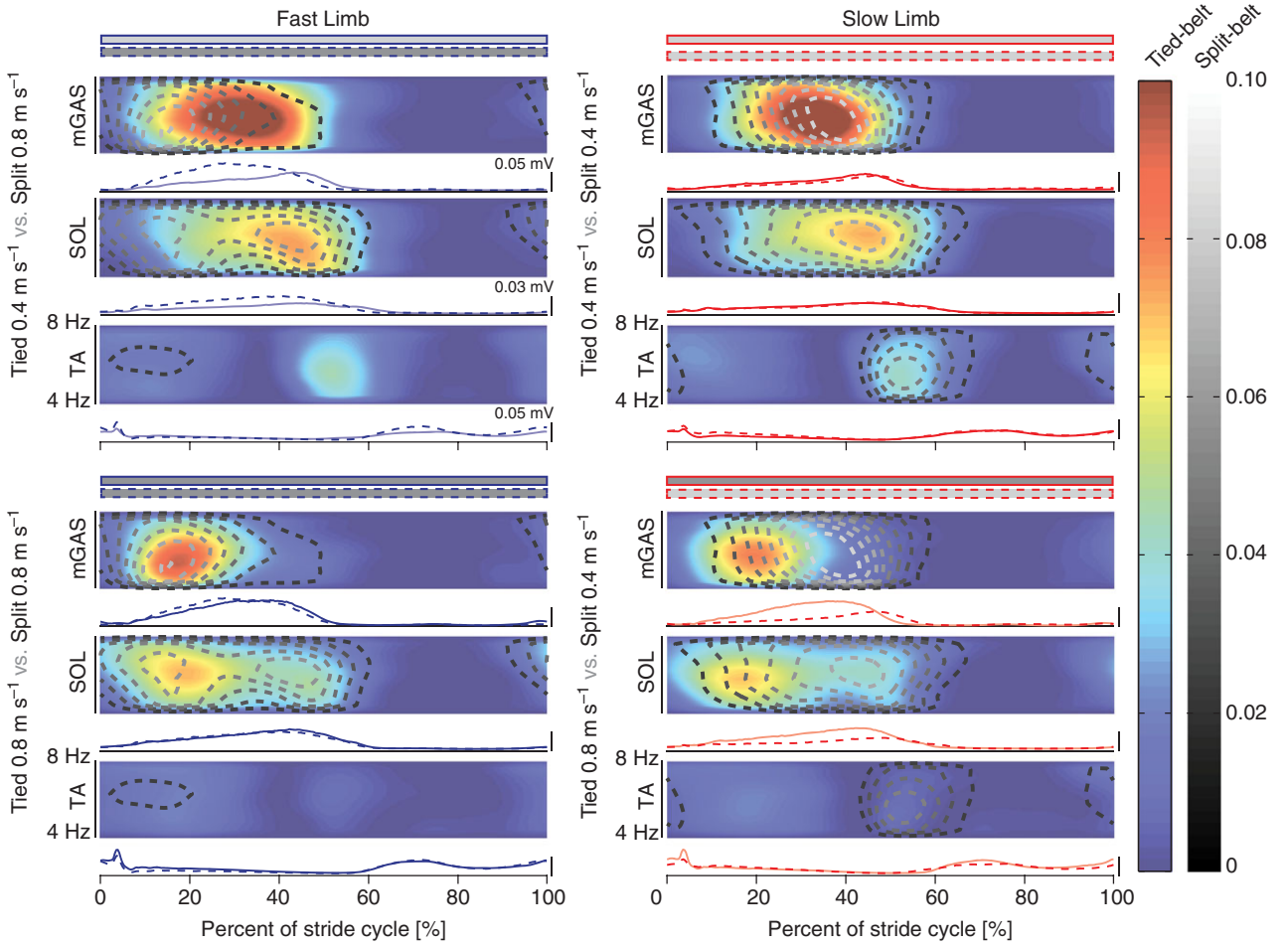

Figure 3. Mean coherence and EMG ($n = 16$) plotted for each muscle in each limb for all three conditions
Coloured surface plots represent tied-belt responses from each limb and were plotted with desaturated colours. The steady-state split-belt responses are replicated on each row and plotted on top of both 0.4 and 0.8 m s^{-1} tied-belt conditions as black and white contour lines to highlight the similarities and differences between the three conditions. EMG signals under each coherence plot show the mean muscle activity from the same muscle across the two conditions being compared. Fast limb split-belt responses were similar to the 0.8 m s^{-1} tied-belt responses, and slow limb split-belt responses were similar to the 0.4 m s^{-1} tied-belt responses. For illustrative purposes, coherence was plotted over a limited bandwidth (4–8 Hz) where peak responses are typically observed. Colour and grey vertical bars indicate the coherence magnitude for tied-belt and split-belt conditions, respectively, and for illustrative purposes data below the $P = 0.01$ confidence limit have been set to zero. Because the mean peak coherence in time–frequency plots washes out with averaging due to variance in response timing, the scale of the colour and grey plotting has been limited to 0.1 to improve the display. All data are aligned to the heel strike of each limb separately. Horizontal grey bars above each coherence plot are used to represent the different condition and limb combinations as depicted in Figs 1 and 2.

muscles and Fig. 6 for mGAS responses). Furthermore, for the other two muscles, we observed no obvious initial change in coherence at the start of split-belt walking (Table 1). The timing of peak coherence and peak EMG always occurred earlier in the stride cycle for the fast limb as compared to the slow limb, and both coherence and EMG timing reached values similar to their respective tied-belt and steady-state split-belt responses within each limb (Fig. 6*B* and *C*). However, the changes in peak coherence timing in all muscles occurred almost immediately (i.e. 13 strides) following the onset of split-belt walking, and contrasted with the gradual change in peak EMG timing that required a greater number of strides to plateau (~20–70 strides) (see Table 1 for all muscles and Fig. 6 for mGAS responses).

During the post-adaptation phase, there were no obvious lasting effects of split-belt adaptation on vestibulo-muscular responses. Both the coherence magnitude and timing for all muscles returned to 0.4 m s^{-1} tied-belt levels within 13–22 strides (see Table 1 for all muscles and Fig. 6*C* for mGAS responses). Although immediate changes in step symmetry, iEMG and peak EMG timing were also observed at the onset of the post-adaptation phase, their progressive convergence to 0.4 m s^{-1} tied-belt levels occurred over a longer time course (~85, 20–80 and 20–40 strides, respectively) relative to the changes observed in coherence. Overall, these results indicate that vestibulo-muscular coupling is rapidly modulated during locomotor adaptation, and is not entirely dependent upon general changes in EMG magnitude and timing.

Discussion

The primary aim of this study was to determine whether the vestibular contribution to lower limb muscles during locomotion is independently or bilaterally modulated with limb velocity. Subjects walked at a fixed cadence in order to match leg kinematics and muscle activity in each limb during split-belt walking to velocity-matched tied-belt conditions. Under this constraint, we found that the magnitude and timing of vestibular contributions to each limb during steady-state split-belt walking was similar to its velocity-matched tied-belt condition. These results suggest that the vestibular influence on lower limb muscle activity is maintained through independent limb-specific control rather than bilaterally coordinated mechanisms.

Our data also demonstrate that the adaptation of vestibulo-motor response magnitude (i.e. peak coherence) to split-belt walking was established rapidly following the onset of split-belt walking, much faster than the adaptation time course required for step symmetry or muscle activity amplitude to plateau (13–34 *vs.* 128 or 40–100 strides, respectively). Similarly, the adaptation of vestibulo-motor response timing occurred immediately during split-belt walking, while changes in peak EMG

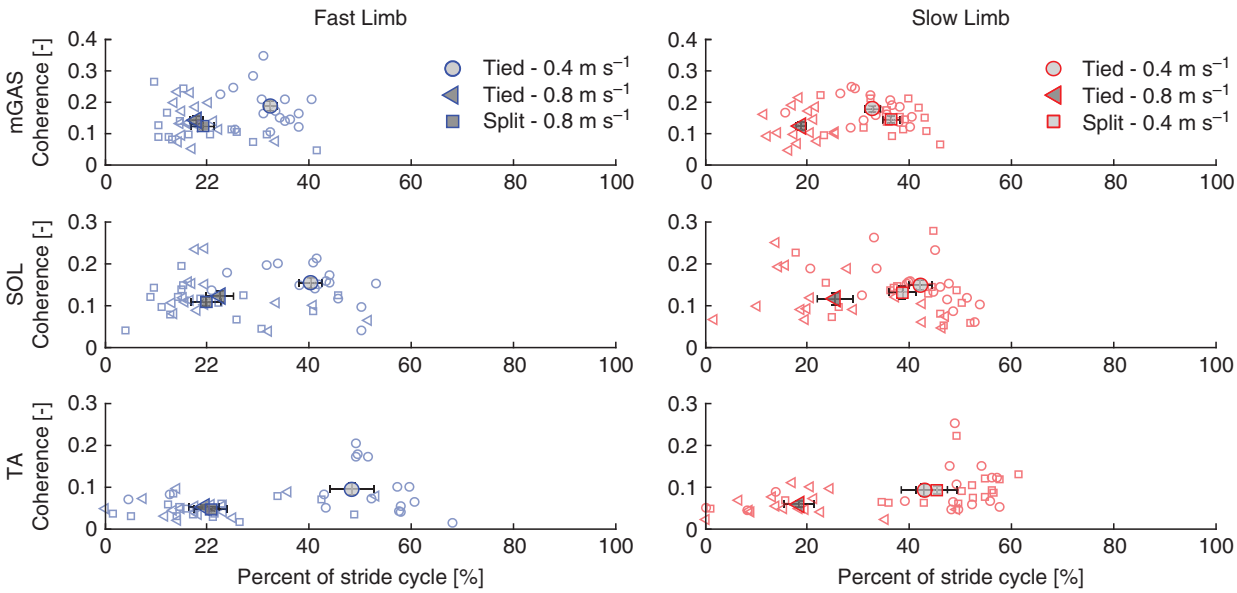

Figure 4. Peak coherence magnitude and timing for each limb across trial conditions
In the fast limb (blue), split-belt responses (square symbols) tend to cluster closer to the 0.8 m s^{-1} velocity-matched tied-belt responses (triangle symbols), and in the slow limb (red), split-belt responses (square symbols) tend to cluster closer to the 0.4 m s^{-1} velocity-matched tied-belt responses (circle symbols). Timing data are aligned relative to the heel strike of each limb separately. Open symbols indicate each subject's response, and filled symbols indicate the group mean. The filled shading of the group means reflects the belt velocity (either 0.8 m s^{-1}: dark grey, or 0.4 m s^{-1}: light grey) at which each limb moved, similar to the horizontal bars used in Figs 1–3. Error bars indicate SEM ($n = 16$).

Table 3. Summary of peak coherence magnitude and timing obtained from all muscles in all conditions

		Coherence peak magnitude			Coherence peak timing (% of stride cycle)		
		Tied-belt 0.4 m s^{-1}	Tied-belt 0.8 m s^{-1}	Split-belt	Tied-belt 0.4 m s^{-1}	Tied-belt 0.8 m s^{-1}	Split-belt
Fast limb	mGAS	0.19 ± 0.02	0.14 ± 0.01	0.12 ± 0.02	32.3 ± 1.3	17.8 ± 1.2	19.1 ± 2.2
	SOL	0.15 ± 0.01	0.12 ± 0.01	0.11 ± 0.01	40.2 ± 2.2	22.4 ± 2.8	19.8 ± 2.9
	TA	0.09 ± 0.01	0.05 ± 0.01	0.05 ± 0.01	48.4 ± 4.2	19.4 ± 3.0	20.8 ± 4.1
Slow limb	mGAS	0.18 ± 0.01	0.13 ± 0.01	0.15 ± 0.01	32.7 ± 1.6	18.7 ± 1.0	36.3 ± 1.7
	SOL	0.15 ± 0.01	0.12 ± 0.01	0.14 ± 0.01	42.1 ± 2.2	25.4 ± 3.5	38.6 ± 2.6
	TA	0.09 ± 0.01	0.06 ± 0.01	0.09 ± 0.01	42.8 ± 4.6	18.3 ± 2.9	45.2 ± 3.1

The fast and slow limb designations were defined based on the split-belt condition; during tied-belt conditions both limbs (slow and fast) moved at the same speed (i.e. 0.4 or 0.8 m s^{-1}) while their designations of 'slow' and 'fast' are maintained for comparison with split-belt responses. Magnitude and timing values are means ± SEM ($n = 16$).

timing occurred over a more prolonged time course (0–13 *vs.* 20–70 strides). There were also no lasting effects of split-belt walking on vestibulo-muscular coupling during the post-adaptation phase. These findings suggest that the vestibular modulation of lower limb muscle activity does not adapt via the same forward model mechanisms presumed to contribute to step symmetry and muscle activity adaptation during split-belt walking. They also indicate that these vestibulo-muscular changes are not simply due to general changes in the magnitude or timing of muscle activity. Instead, the rapid adjustment of EVS–EMG coherence indicates that local sensory feedback mechanisms guide the vestibular contribution to locomotor activity.

Rapid limb-specific modulation of vestibulo-muscular coupling during split-belt walking through sensory feedback control

The similarity of vestibulo-muscular coupling during steady-state split-belt walking to each limb's velocity-matched tied-belt response provides evidence that vestibular contributions to locomotor activity of each limb are modulated independently. This independent modulation may be advantageous when adapting to asymmetric changes in locomotion, such as turning or walking on uneven terrain. As one limb moves slower, vestibular contributions can be maintained in the opposing limb without compromising ongoing motor patterns. Similar forms of limb-specific control during split-belt walking have been observed previously: when subjects (adults and infants) walk with the limbs moving in opposite directions (i.e. one forward and one backward) the limbs can adapt separately, whereby the after-effects of adaptation are stored individually for each limb (Yang *et al.* 2005; Choi & Bastian, 2007). Central pattern generators (CPGs) in animals (Grillner, 1979; Kiehn, 2006), and possibly in humans (Calancie *et al.* 1994; Dimitrijevic *et al.* 1998; Dominici *et al.* 2011), are thought to produce and maintain the separate rhythm and pattern of locomotion in each limb. Support for the independence of these neural networks can be seen in human infants (Yang *et al.* 2005) and spinalized cats (Forssberg *et al.* 1980), both of which can make multiple steps in the fast limb (sometimes up to four in cats) during a single step cycle in the slow limb. Each network is suggested to be controlled and modulated by descending motor commands and sensory feedback from afferent inputs (see reviews by Rossignol *et al.* 2006; McCrea & Rybak, 2008), including contributions from descending vestibular signals (Ten Bruggencate & Lundberg, 1974; Leblond & Gossard, 1997; Leblond *et al.* 1998). In the present study, we demonstrate that the vestibular signals modulate independently the locomotor activity within each limb depending on its movement velocity. Therefore, we speculate that vestibular signals interact with the separate neural networks for each limb that are involved in (split-belt) locomotion.

The potential interaction between vestibular input and limb-specific locomotor networks appears to occur primarily through sensory feedback mechanisms rather than predictive feedforward processes that involve progressive updating of a forward model. This is because limb-specific changes in EVS–EMG coherence during split-belt walking occurred relatively quickly, within 13–34 strides, and we observed no lasting effects on peak coherence magnitude or timing during the post-adaptation phase. This rapid adaptation parallels the observation that heading errors immediately decrease in patients with vestibular deficits (neuritis) and healthy subjects during EVS when running compared to walking (Brandt *et al.* 1999; Brandt, 2000; Jahn *et al.* 2000). They also align with the reported time scales (<30 s) required for the balance system to recognize a discrepancy between vestibular and motor signals (<1 s; Luu *et al.* 2012) or re-associate modified relationships between these two signals (<30 s; Forbes *et al.* 2016). In animals, feedback-driven adaptations are seen in both intact and spinalized cats when the hindlimbs are set to walk on a

Table 4. Summary of statistical tests performed on peak coherence magnitude and timing results (Table 3) obtained from all muscles

		MANOVA and *post hoc* results										
		Walking condition		0.4 m s^{-1} *vs.* 0.8 m s^{-1} tied-belt			Split- *vs.* tied-belt: unmatched			Split- *vs.* tied-belt: matched		
					Univariate			Univariate			Univariate	
		$F_{4,12}$	P	Multi-variate	Magnitude	Timing	Multi-variate	Magnitude	Timing	Multi-variate	Magnitude	Timing
Fast limb	mGAS	23.05	<0.001	<0.001	0.023	<0.001	<0.001	<0.001	<0.001	*0.084*	–	–
	SOL	32.11	<0.001	<0.001	0.029	<0.001	<0.001	<0.001	<0.001	*0.747*	–	–
	TA	21.91	<0.001	<0.001	0.02	<0.001	<0.001	0.008	<0.001	*0.526*	–	–
Slow limb	mGAS	69.87	<0.001	<0.001	<0.001	<0.001	<0.001	0.043	<0.001	0.002	0.001	*0.153*
	SOL	8.49	0.002	<0.001	*0.098*	<0.001	0.015	*0.444*	0.003	*0.110*	–	–
	TA	8.75	0.002	<0.001	0.026	<0.001	<0.001	0.006	0.001	*0.812*	–	–

The fast and slow limb designations were defined based on the split-belt condition; during tied-belt conditions both limbs (slow and fast) moved at the same speed (i.e. 0.4 or 0.8 m s^{-1}) while their designations of 'slow' and 'fast' are maintained for comparison with split-belt responses. The italicized values represent effects that were not significant.

split-belt treadmill (Forssberg *et al.* 1980; Frigon *et al.* 2013). Stance and swing times are modified immediately in both animal preparations, suggesting that asymmetric sensory feedback evoked by differing limb velocities alters the excitability of neuronal networks within the spinal cord controlling each limb (Frigon *et al.* 2013). Predictive feed-forward adaptations, in contrast, occur through continued exposure to split-belt walking over a longer time course and lead to aftereffects (Morton & Bastian, 2006; Malone & Bastian, 2010). Here, step symmetry, iEMG and peak EMG timing plateaued in split-belt walking after approximately 128, 40–100 and 20–70 strides, respectively, and washed out during post-adaptation walking after approximately 89, 20–80 and 20–40 strides, respectively. From a functional perspective, it seems sensible that vestibular sensorimotor adaptation for locomotion precedes changes in muscle activity and subsequent kinematics; sensory information that is adapted to the locomotion task can drive effective changes in muscle activity and related kinematic responses.

Neural substrates for limb-specific sensory feedback modulation of vestibulo-muscular coupling

There are several neural structures that could mediate the observed changes in vestibular drive to lower limb muscle activity and their contributions may not be mutually exclusive. Centrally, cortical activity associated with vestibular sensory processing progressively decreases during imagined walking and running relative to imagined standing (Jahn *et al.* 2004), while subcortical activity, thought to be associated with the supraspinal control of locomotion, progressively increases (Jahn *et al.* 2008). It remains unclear, however, whether these brain regions exhibit similar velocity-dependent changes during real *versus* imagined walking. The vestibular nucleus (VN) is a potential site for subcortical modulation as it integrates both vestibular and proprioceptive signals. VN neurons in alert cats modulate in phase with limb kinematics and are thought to govern the extensor muscle activity to counter gravity (Orlovsky, 1972; Matsuyama & Drew, 2000*a*, *b*). Discharge patterns in VN neurons also depend on the overall pattern of inter-limb coordination and/or the pattern of activity in a specific limb (Matsuyama & Drew, 2000*a*), the latter observation parallelling the results of our study. Moreover, VN neurons that are excited by hindlimb flexion most often increase firing rate during ipsilateral roll rotations, whereas neurons that are excited by hindlimb extension increase firing rate during contralateral head roll (Arshian *et al.* 2014). This directional specificity of VN neurons to both vestibular and limb input signals suggests that their integration is functionally relevant (Arshian *et al.* 2014), and could be a neural substrate for the limb-specific vestibulo-muscular modulation seen here.

Peripherally, descending vestibular signals may be modulated through local spinal circuits according to limb-specific somatosensory information. During split-belt walking in humans and animals, somatosensory feedback from limb receptors is thought to contribute to normal and adapted locomotion by modulating the activity of the local spinal circuitry (i.e. CPGs) (Forssberg *et al.* 1980; Dietz *et al.* 1994; Prokop *et al.* 1995; Rossignol *et al.* 2006; Frigon *et al.* 2013). The interaction of these locomotor circuits with vestibular signals in animal studies, however, can yield conflicting interpretations. In cats, vestibulospinal tracts and extensor afferents converge on flexor afferent spinal pathways (Ten Bruggencate & Lundberg, 1974; Leblond & Gossard, 1997), while their convergence on polysynaptic excitatory pathways to extensor muscles is absent (Leblond & Gossard, 1997). In the current study, in contrast, we observed velocity-dependent modulation of both dorsi-flexor (TA) and plantar-flexor (SOL and mGAS) ankle muscles. For humans, vestibular input interacts with the transmission of muscle afferent spinal pathways (facilitating reciprocal Ia inhibition, group I non-reciprocal inhibition and Ia presynaptic inhibitions) (Rossi *et al.* 1988; Iles & Pisini, 1992; Kennedy & Inglis, 2002) as well as cutaneous afferent spinal pathways (Muise *et al.* 2012; Thomas & Bent, 2013). These findings therefore support the existence of the spinal afferent circuits that are at least capable of modulating descending vestibulospinal pathways. However, because the present results cannot identify the specific circuits (i.e. VN neurons *vs.* spinal neurons) involved with the vestibulo-muscular modulation observed here, further human and animal testing would be needed.

Coherence timing, in addition to magnitude, is modulated with limb velocity during tied- and split-belt conditions

In addition to decreasing coherence magnitude (Dakin *et al.* 2013), increasing locomotor velocity advanced the timing of peak vestibulo-muscular coupling by ~180–380 ms (12–25%) in the stride cycle in both tied- and split-belt conditions. Vestibular contributions to ankle muscle activity earlier in the stance phase may be beneficial to compensate for the reduced stance time where the muscles in the fast limb can influence the control of balance during locomotion. Because weight transfer (i.e. loading) to the stance limb occurs earlier in the locomotion cycle when the limb is moving faster (see Z-forces in

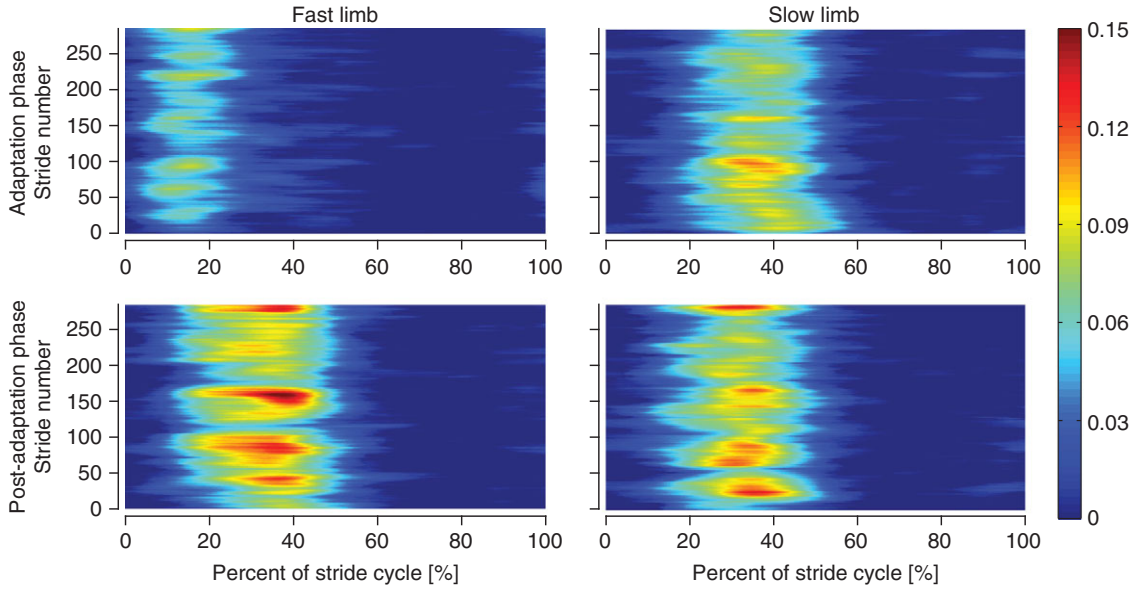

Figure 5. Stride-by-stride mean coherence estimated from the group-pooled mGAS muscle responses of all subjects (n = 16). Responses shown are during the adaptation phase (top) of split-belt walking and post-adaptation tied-belt walking (bottom)
Coherence for each stride was estimated using a window of 15 strides from all 16 subjects for a total of 240 strides per window. For illustrative purposes, the coherence for each stride was plotted over a limited bandwidth (4–8 Hz) where peak responses are typically observed. Coherence magnitude is indicated by the colour bars and data below the $P = 0.01$ confidence limit have been set to zero for illustrative purposes. After the onset of split-belt walking, coherence magnitude and timing were established rapidly and were similar to the responses estimated from the velocity-matched tied belt conditions for each limb (i.e. slow limb = 0.4 m s^{-1} and fast limb = 0.8 m s^{-1}). Subsequently, there were no lasting affects in the coherence responses during post-adaptation tied-belt walking and the magnitude and timing rapidly returned to normal tied-belt 0.4 m s^{-1} responses. All data are aligned to the heel strike of each limb separately.

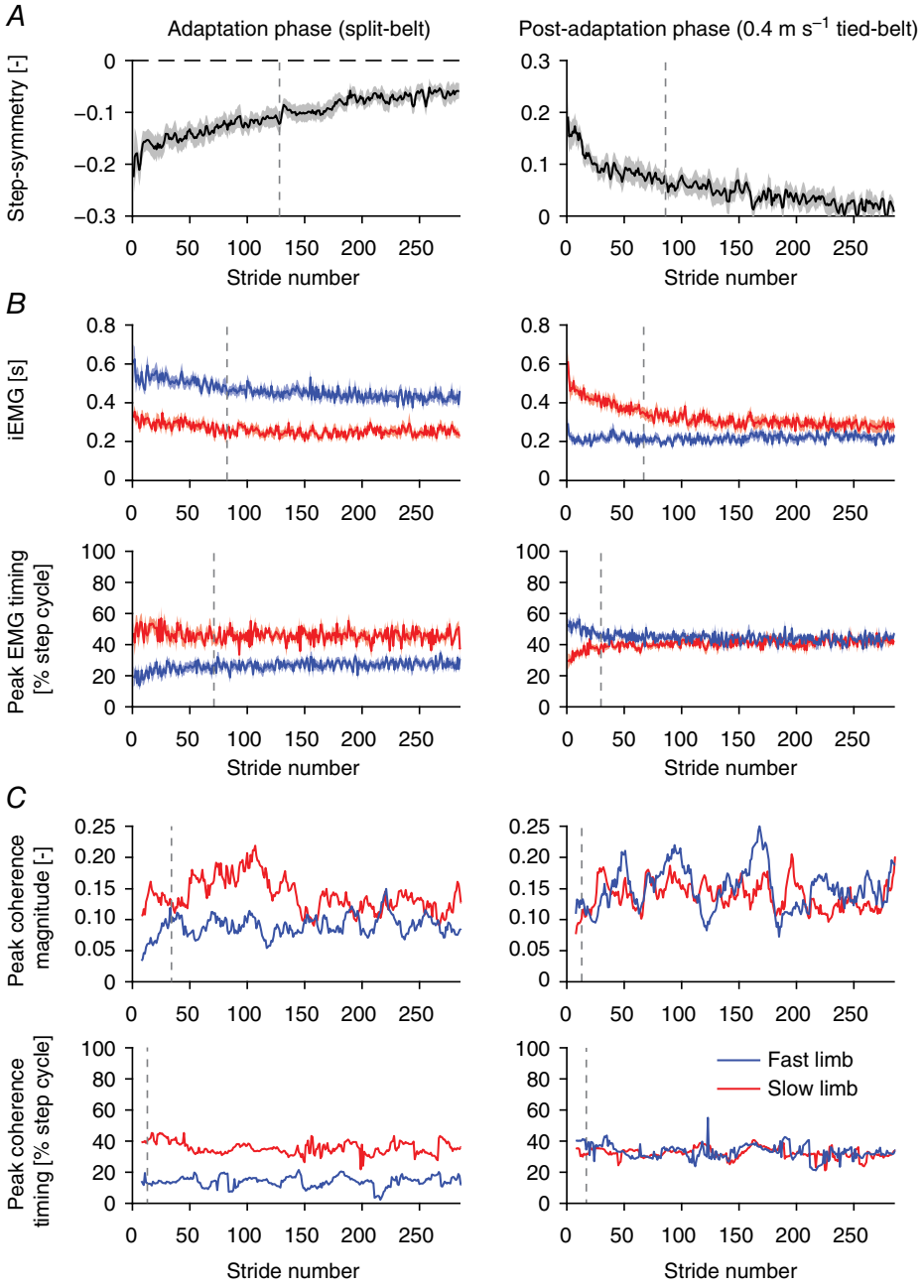

Figure 6. Comparison of mean stride-by-stride step symmetry (n = 16), mean mGAS magnitude (integrated EMG) and timing (peak EMG) (n = 16), and pooled group mGAS peak coherence magnitude and timing during the adaptation phase of split-belt walking and post-adaptation tied-belt walking
A, step symmetry is in the opposite direction across the adaptation and post-adaptation phases. Shaded areas represent the SEM (n = 16). *B*, integrated EMG and peak EMG timing are progressively modulated throughout the adaptation and post-adaptation phases. Shaded areas represent the SEM (n = 16). *C*, peak mean coherence magnitude and timing were extracted from each stride of the group-pooled coherence estimate over the entire frequency bandwidth (0–25 Hz). The group-pooled coherence was estimated from the group-pooled responses of all subjects (n = 16) over a window of 15 strides for a total of 240 strides per window. Timing data are aligned relative to the heel strike of each limb separately. Vertical lines indicate when adaptation was complete using the duration of adaptation estimate (see Methods). mGAS, medial gastrocnemius.

Fig. 1*C*), the influence of load-related afferent feedback could, at least in part, be responsible for the advance timing in EVS–EMG coherence (Marsden *et al.* 2002, 2003). However, this is probably not the only contributing factor because the advancement of peak coherence did not match the reduction in stance time (~90 ms). Another possible explanation may relate to the earlier rise and larger peak in fast limb muscle activity in the stance phase, which may advance the vestibular contribution within the stride cycle (see Fig. 1*C*, mGAS and SOL EMG signals). The activation of a muscle, along with its engagement in balance control, is a prerequisite to generate vestibular-evoked responses in appendicular muscles throughout the body (Britton *et al.* 1993; Fitzpatrick *et al.* 1994; Luu *et al.* 2012; Forbes *et al.* 2015). Our results suggest, however, that the advanced timing (and magnitude) of EMG levels are unlikely to be a cause for the observed decrease in coherence. First, peak EMG does not always align with peak coherence (see Fig. 3 mGAS and TA responses and Blouin *et al.* 2011) and, second, changes in the timing of peak coherence during split-belt walking exhibited a more rapid time course compared to changes in peak EMG timing (see Fig. 6).

Alternatively, previous studies have suggested that the timing of vestibulo-muscular coupling may reflect the functional role of a muscle in responding to the medio-lateral vestibular perturbation (Blouin *et al.* 2011), such as ankle stabilization prior to push off or mediolateral placement of the contralateral foot (Bent *et al.* 2004; Blouin *et al.* 2011). Following a similar argument, we suggest that the advanced timing of peak coherence at higher belt velocities may partially compensate for the reduced magnitude in vestibulo-muscular coupling by contributing to medio-lateral postural control earlier in the stride cycle. Whether the magnitude and timing changes observed here reflect different underlying mechanisms cannot be determined from our current results. Nevertheless, we suggest that these two factors (magnitude and timing) are coordinated such that the vestibular influence on a muscle is maintained when it is most beneficial to the lateral stabilization of locomotion. The results of this study indicate that the organization (i.e. magnitude and timing) of vestibulo-motor coupling is retained separately for each limb even when the limbs are moving at different velocities.

Methodological considerations

The use of a metronome to control cadence may limit the parallels drawn between our results and other split-belt studies. Compared to traditional split-belt studies, where cadence is unconstrained, the number of strides required for step symmetry to plateau was smaller (~128 *vs.* ~175 strides; Malone & Bastian, 2010). Instead, the duration of adaptation in our metronome-controlled split-belt walking was comparable to conditions where subjects consciously correct for asymmetries in split-belt walking (~128 *vs.* ~100 strides; Malone & Bastian, 2010). Nevertheless, the observed plateau indicated that adaptation was still required even with the added metronome constraint and that subjects had fully adapted prior to the steady-state phase of split-belt walking (i.e. 8–16 min). Control for cadence, however, was necessary. When subjects were free to walk at their preferred cadence (see Methods), their cadences varied across the tied-belt and split-belt conditions. These condition-dependent variations in limb kinematics introduced confounding factors when comparing vestibulo-muscular coupling across conditions on account of its sensitivity to both locomotor velocity and cadence (Dakin *et al.* 2013). Our results indicate that by controlling cadence, the limb kinematics and EMG profile within each limb during split-belt walking corresponded closely to the velocity-matched tied-belt condition. More importantly, under these constraints, changes in limb locomotor velocity induced alterations in the vestibular contribution to locomotor activity.

Conclusions

We have shown that the vestibular contribution to lower limb muscle activity can be independently modulated. During split-belt walking, vestibulo-muscular peak coherence within each limb retains similar magnitude and timing relative their tied-belt velocity-matched condition. At the onset of, and immediately following, split-belt walking, this limb-specific modulation occurs much faster than the adaptation of a forward model for error correction that is presumed to drive changes in muscle activity and step symmetry. Together, these findings demonstrate the CNS's ability to separately modulate the vestibular contribution to each limb during locomotion, a process which is probably facilitated through afferent feedback loops. Limb-specific vestibulo-motor control through ongoing sensorimotor loops may be advantageous in accommodating the variable and asymmetric demands of overground locomotion such as navigating irregular terrain or turning.

References

Arshian MS, Hobson CE, Catanzaro MF, Miller DJ, Puterbaugh SR, Cotter LA, Yates BJ & McCall AA (2014). Vestibular nucleus neurons respond to hindlimb movement in the decerebrate cat. *J Neurophysiol* **111**, 2423–2432.

Bent LR, Inglis JT & McFadyen BJ (2004). When is vestibular information important during walking? *J Neurophysiol* **92**, 1269–1275.

Blouin J-S, Dakin CJ, van den Doel K, Chua R, McFadyen BJ & Inglis JT (2011). Extracting phase-dependent human vestibular reflexes during locomotion using both time and frequency correlation approaches. *J Appl Physiol* **111**, 1484–1490.

Brandt T (2000). Vestibulopathic gait: you're better off running than walking. *Curr Opin Neurol* **13**, 3–5.

Brandt T, Strupp M & Benson J (1999). You are better off running than walking with acute vestibulopathy. *Lancet* **354**, 746–746.

Britton TC, Day BL, Brown P, Rothwell JC, Thompson PD & Marsden CD (1993). Postural electromyographic responses in the arm and leg following galvanic vestibular stimulation in man. *Exp Brain Res* **94**, 143–151.

Calancie B, Needhamshropshire B, Jacobs P, Willer K, Zych G & Green BA (1994). Involuntary stepping after chronic spinal cord injury. Evidence for a central rhythm generator for locomotion in man. *Brain* **117**, 1143–1159.

Cathers I, Day BL & Fitzpatrick RC (2005). Otolith and canal reflexes in human standing. *J Physiol* **563**, 229–234.

Choi JT & Bastian AJ (2007). Adaptation reveals independent control networks for human walking. *Nat Neurosci* **10**, 1055–1062.

Cohen B, Yakushin SB & Holstein GR (2012). What does galvanic vestibular stimulation actually activate: response. *Front Neurol* **3**, 148–148.

Curthoys IS & Macdougall HG (2012). What galvanic vestibular stimulation actually activates. *Front Neurol* **3**, 117–117.

Dakin CJ, Dalton BH, Luu BL & Blouin JS (2014). Rectification is required to extract oscillatory envelope modulation from surface electromyographic signals. *J Neurophysiol* **112**, 1685–1691.

Dakin CJ, Inglis JT, Chua R & Blouin JS (2013). Muscle-specific modulation of vestibular reflexes with increased locomotor velocity and cadence. *J Neurophysiol* **110**, 86–94.

Dakin CJ, Luu BL, van den Doel K, Inglis JT & Blouin JS (2010). Frequency-specific modulation of vestibular-evoked sway responses in humans. *J Neurophysiol* **103**, 1048–1056.

Dakin CJ, Son GML, Inglis JT & Blouin JS (2007). Frequency response of human vestibular reflexes characterized by stochastic stimuli. *J Physiol* **583**, 1117–1127.

Day BL & Fitzpatrick RC (2005). Virtual head rotation reveals a process of route reconstruction from human vestibular signals. *J Physiol* **567**, 591–597.

Dietz V, Zijlstra W & Duysens J (1994). Human neuronal interlimb coordination during split-belt locomotion. *Exp Brain Res* **101**, 513–520.

Dimitrijevic MR, Gerasimenko Y & Pinter MM (1998). Evidence for a spinal central pattern generator in humans. In *Neuronal Mechanisms for Generating Locomotor Activity*, eds. Kiehn O, HarrisWarrick RM, Jordan LM, Hultborn H & Kudo N, pp. 360–376. New York Academy of Sciences, New York.

Dominici N, Ivanenko YP, Cappellini G, d'Avella A, Mondi V, Cicchese M, Fabiano A, Silei T, Di Paolo A, Giannini C, Poppele RE & Lacquaniti F (2011). Locomotor primitives in newborn babies and their development. *Science* **334**, 997–999.

Finley JM, Bastian AJ & Gottschall JS (2013). Learning to be economical: the energy cost of walking tracks motor adaptation. *J Physiol* **591**, 1081–1095.

Fitzpatrick R, Burke D & Gandevia SC (1994). Task-dependent reflex responses and movement illusions evoked by galvanic vestibular stimulation in standing humans. *J Physiol* **478**, 363–372.

Fitzpatrick RC, Butler JE & Day BL (2006). Resolving head rotation for human bipedalism. *Curr Biol* **16**, 1509–1514.

Fitzpatrick RC & Day BL (2004). Probing the human vestibular system with galvanic stimulation. *J Appl Physiol* **96**, 2301–2316.

Forbes PA, Luu BL, Van der Loos HF, Croft EA, Inglis JT & Blouin JS (2016). Transformation of vestibular signals for the control of standing in humans. *J Neurosci* **36**, 11510–11520.

Forbes PA, Siegmund GP, Happee R, Schouten AC & Blouin JS (2014). Vestibulocollic reflexes in the absence of head postural control. *J Neurophysiol* **112**, 1692–1702.

Forbes PA, Siegmund GP, Schouten AC & Blouin JS (2015). Task, muscle and frequency dependent vestibular control of posture. *Front Integr Neurosci* **8**, 94.

Forssberg H, Grillner S, Halbertsma J & Rossignol S (1980). The locomotion of the low spinal cat. II. Interlimb coordination. *Acta Physiol Scand* **108**, 283–295.

Frigon A, Hurteau MF, Thibaudier Y, Leblond H, Telonio A & D'Angelo G (2013). Split-belt walking alters the relationship between locomotor phases and cycle duration across speeds in intact and chronic spinalized adult cats. *J Neurosci* **33**, 8559–8566.

Goldberg JM, Smith CE & Fernandez C (1984). Relation between discharge regularity and responses to externally applied galvanic currents in vestibular nerve afferents of the squirrel-monkey. *J Neurophysiol* **51**, 1236–1256.

Grillner S (1979). Interaction between central and peripheral mechanisms in the control of locomotion. *Prog Brain Res* **50**, 227–235.

Iles JF, Baderin R, Tanner R & Simon A (2007). Human standing and walking: comparison of the effects of stimulation of the vestibular system. *Exp Brain Res* **178**, 151–166.

Iles JF & Pisini JV (1992). Vestibular-evoked postural reactions in man and modulation of transmission in spinal reflex pathways. *J Physiol* **455**, 407–424.

Ivanenko YP, Poppele RE & Lacquaniti F (2006). Motor control programs and walking. *Neuroscientist* **12**, 339–348.

Jahn K, Deutschlander A, Stephan T, Kalla R, Wiesmann M, Strupp M & Brandt T (2008). Imaging human supraspinal locomotor centers in brainstem and cerebellum. *Neuroimage* **39**, 786–792.

Jahn K, Deutschlander A, Stephan T, Strupp M, Wiesmann M & Brandt T (2004). Brain activation patterns during imagined stance and locomotion in functional magnetic resonance imaging. *Neuroimage* **22**, 1722–1731.

Jahn K, Strupp M, Schneider E, Dieterich M & Brandt T (2000). Differential effects of vestibular stimulation on walking and running. *Neuroreport* **11**, 1745–1748.

Kawato M, Furukawa K & Suzuki R (1987). A hierarchical neural-network model for control and learning of voluntary movement. *Biol Cybern* **57**, 169–185.

Kennedy PM & Inglis JT (2002). Interaction effects of galvanic vestibular stimulation and head position on the soleus H reflex in humans. *Clin Neurophysiol* **113**, 1709–1714.

Kiehn O (2006). Locomotor circuits in the mammalian spinal cord. *Annu Rev Neurosci* **29**, 279–306.

Kim J & Curthoys IS (2004). Responses of primary vestibular neurons to galvanic vestibular stimulation (GVS) in the anaesthetised guinea pig. *Brain Res Bull* **64**, 265–271.

Leblond H & Gossard JP (1997). Supraspinal and segmental signals can be transmitted through separate spinal cord pathways to enhance locomotor activity in extensor muscles in the cat. *Exp Brain Res* **114**, 188–192.

Leblond H, Menard A & Gossard JP (1998). Vestibulo- and reticulospinal control of the extensor half-center in locomotion. *Ann NY Acad Sci* **860**, 563–565.

Lund S & Broberg C (1983). Effects of different head positions on postural sway in man induced by a reproducible vestibular error signal. *Acta Physiol Scand* **117**, 307–309.

Luu BL, Inglis JT, Huryn TP, Van der Loos HFM, Croft EA & Blouin J-S (2012). Human standing is modified by an unconscious integration of congruent sensory and motor signals. *J Physiol* **590**, 5783–5794.

MacLellan MJ, Ivanenko YP, Massaad F, Bruijn SM, Duysens J & Lacquaniti F (2014). Muscle activation patterns are bilaterally linked during split-belt treadmill walking in humans. *J Neurophysiol* **111**, 1541–1552.

Malone LA & Bastian AJ (2010). Thinking about walking: effects of conscious correction versus distraction on locomotor adaptation. *J Neurophysiol* **103**, 1954–1962.

Marsden JF, Blakey G & Day BL (2003). Modulation of human vestibular-evoked postural responses by alterations in load. *J Physiol* **548**, 949–953.

Marsden JF, Castellote J & Day BL (2002). Bipedal distribution of human vestibular-evoked postural responses during asymmetrical standing. *J Physiol* **542**, 323–331.

Matsuyama K & Drew T (2000*a*). Vestibulospinal and reticulospinal neuronal activity during locomotion in the intact cat. I. Walking on a level surface. *J Neurophysiol* **84**, 2237–2256.

Matsuyama K & Drew T (2000*b*). Vestibulospinal and reticulospinal neuronal activity during locomotion in the intact cat. II. Walking on an inclined plane. *J Neurophysiol* **84**, 2257–2276.

McCrea DA & Rybak IA (2008). Organization of mammalian locomotor rhythm and pattern generation. *Brain Res Rev* **57**, 134–146.

Mian OS, Dakin CJ, Blouin J-S, Fitzpatrick RC & Day BL (2010). Lack of otolith involvement in balance responses evoked by mastoid electrical stimulation. *J Physiol* **588**, 4441–4451.

Mian OS & Day BL (2014). Violation of the craniocentricity principle for vestibularly evoked balance responses under conditions of anisotropic stability. *J Neurosci* **34**, 7696–7703.

Misiaszek JE (2006). Neural control of walking balance: if falling then react else continue. *Exerc Sport Sci Rev* **34**, 128–134.

Morton SM & Bastian AJ (2006). Cerebellar contributions to locomotor adaptations during splitbelt treadmill walking. *J Neurosci* **26**, 9107–9116.

Muise SB, Lam CK & Bent LR (2012). Reduced input from foot sole skin through cooling differentially modulates the short latency and medium latency vestibular reflex responses to galvanic vestibular stimulation. *Exp Brain Res* **218**, 63–71.

Olree KS & Vaughan CL (1995). Fundamental patterns of bilateral muscle activity in human locomotion. *Biol Cybern* **73**, 409–414.

Orlovsky GN (1972). Activity of vestibulospinal neurons during locomotion. *Brain Res* **46**, 85–98.

Pandy MG, Lin Y-C & Kim HJ (2010). Muscle coordination of mediolateral balance in normal walking. *J Biomech* **43**, 2055–2064.

Peters RM, Rasman BG, Inglis JT & Blouin JS (2015). Gain and phase of perceived virtual rotation evoked by electrical vestibular stimuli. *J Neurophysiol* **114**, 264–273.

Prokop T, Berger W, Zijlstra W & Dietz V (1995). Adaptational and learning processes during human split-belt locomotion: interaction between central mechanisms and afferent input. *Exp Brain Res* **106**, 449–456.

Reisman DS, Block HJ & Bastian AJ (2005). Interlimb coordination during locomotion: what can be adapted and stored? *J Neurophysiol* **94**, 2403–2415.

Reynolds RF (2010). The effect of voluntary sway control on the early and late components of the vestibular-evoked postural response. *Exp Brain Res* **201**, 133–139.

Reynolds RF (2011). Vertical torque responses to vestibular stimulation in standing humans. *J Physiol* **589**, 3943–3953.

Reynolds RF & Osler CJ (2012). Galvanic vestibular stimulation produces sensations of rotation consistent with activation of semicircular canal afferents. *Front Neurol* **3**, 104–104.

Rossi A, Mazzocchio R & Scarpini C (1988). Changes in Ia reciprocal inhibition from the peroneal nerve to the soleus alpha-motoneurons with different static body positions in man. *Neurosci Lett* **84**, 283–286.

Rossignol S, Dubuc R & Gossard JP (2006). Dynamic sensorimotor interactions in locomotion. *Physiol Rev* **86**, 89–154.

Shadmehr R & Mussa-Ivaldi FA (1994). Adaptive representation of dynamics during learning of a motor task. *J Neurosci* **14**, 3208–3224.

Ten Bruggencate G & Lundberg A (1974). Facilitatory interaction in transmission to motoneurons from vestibulospinal fibers and contralateral primary afferents. *Exp Brain Res* **19**, 248–270.

Thomas KE & Bent LR (2013). Subthreshold vestibular reflex effects in seated humans can contribute to soleus activation when combined with cutaneous inputs. *Motor Control* **17**, 62–74.

Vazquez A, Statton MA, Busgang SA & Bastian AJ (2015). Split-belt walking adaptation recalibrates sensorimotor estimates of leg speed, but not position or force. *J Neurophysiol* **114**, 3255–3267.

Yang JF, Lamont EV & Pang MY (2005). Split-belt treadmill stepping in infants suggests autonomous pattern generators for the left and right leg in humans. *J Neurosci* **25**, 6869–6876.

Zhan Y, Halliday D, Jiang P, Liu X & Feng J (2006). Detecting time-dependent coherence between non-stationary electrophysiological signals – A combined statistical and time-frequency approach. *J Neurosci Methods* **156**, 322–332.

Additional information

Competing interests

All authors have no competing interests.

Author contributions

Experiments in this study were conducted in the Laboratory of Biomechanical Engineering, Institute for Biomedical Technology and Technical Medicine (MIRA), University of Twente. PAF, CJD, JSB and ACS contributed to the conception and design of the experiments. PAF, MV and CJD conducted the experiments. PAF and MV analysed the data. PAF and JSB drafted the manuscript. All authors contributed to the interpretation of the data, critically revising the manuscript and approving the final version to be published.

Funding

This research was supported by the European Union's Seventh Framework Programme for research, technological development and demonstration under the People Programme (Marie Curie Actions – PAF) grant agreement no. 624158 and ICT project no. 610454. JSB received funding from the Natural Sciences and Engineering Research Council of Canada Discovery programme and the Canadian Chiropractic Research Foundation. CJD received funding from the Canadian Institute for Health Research.